Mathematical Problems in Engineering
Volume 5, pp. 361–377
Reprints available directly from the publisher
Photocopying permitted by license only

Exact Solution of Convective Mass Transfer Model for Calcium Response of Endothelium

VINEET KUMAR[a,*], R.N. PANDEY[b] and S.N. UPADHYAY[a,†]

[a]*Department of Chemical Engineering and Technology,* [b]*Department of Applied Mathematics, Institute of Technology, Banaras Hindu University, Varanasi – 221 005, India*

(Received 7 December 1998)

An exact solution for the concentration profile in tubes with surface reaction coupled with permeation have been obtained in terms of fast converging confluent hypergeometric function that gives accurate results. An excellent agreement between the experimental and theoretical results of the intracellular calcium ion concentration in the calf aorta endothelial cells and the extracellular ATP concentration provides yet another example in support of the mass transfer model for intracellular calcium response of the endothelial cells.

Keywords: Endothelium; ATP; Shear stress; Calcium response; Mass transfer; Circular tubes

INTRODUCTION

Vascular endothelium is the simplest epithelium lining the entire vascular system and the only constituent of a capillary wall performing the ultimate function of the entire system, i.e. exchange of nutrients and metabolic end-products of the tissue. To provide strength to a blood vessel, this layer of endothelial cell is supported by layers of elastic tissue, connective tissue, smooth muscles, etc. However, to

* Present address: Thapar Institute of Engineering and Technology, Patiala, Punjab, India.
† Corresponding author. Tel.: 91 542 317192. Fax: 91 542 316925.

facilitate solute transport, no such supporting tissues are present around the endothelial cell layer in capillaries. The structure of a typical capillary is like a thin walled tube made of one layer thick endothelial cells, about 1–2 μm thick and about 20–50 μm in circumferential diameter. To restrict the movement of large protein molecules, these cells are joined together by "tight junctions" [1]. Capillary wall made up of such an arrangement is highly permeable to water and almost all solutes dissolved in blood plasma except protein. Thus it behaves like a semipermeable membrane through which protein free plasma is filtered out. The plasma inside and outside the capillary contains large amount of small molecular weight solutes like Na^+, Cl^-, glucose, etc. Since capillary wall is highly permeable to these molecules, the inside and outside concentrations are almost the same. The permeation and several other physiological characteristics of an endothelial cell depends considerably on the concentration of different constituents in its surrounding fluid [2,3].

To explain such physiological and morphological changes in endothelial cells, a convective mass transfer model has been proposed by various authors. In our earlier communication [4], we have already discussed some of these changes in the endothelial cells due to the presence of different agonists and their degradation (surface reaction) at the cell layer. In that paper the differential equation pertaining to the newly emerging convective mass transfer model for the intracellular calcium response of cultured endothelial cells was solved analytically. The differential equation and velocity profiles used were for the rectangular channel geometry (without permeation) which represent the commonly used experimental set-up for the study of cultured endothelial cells [5–7]. In real situation, however, almost all blood vessels resemble more to a tube having circular cross-section. Also, a few workers [8] have made experiments with cultured endothelial cells supported inside circular glass tubes. Due to this geometry, the differential equation and boundary conditions for the mass transfer model are remarkably different. Due to varying permeation characteristics of endothelium from different parts of the body, it is desirable to have solutions for almost impermeable to highly permeable cases.

In the present paper two processes, surface reaction and permeation through the walls of a tube having circular cross-section, are being considered. The surface reaction is taken to be the degradation of

specific agonist like adenosine triphosphate (ATP) through successive dephosphorylation by three separate actoenzymes [4] and permeation of blood plasma through the endothelium is assumed to be constant throughout the length of the tube.

MATHEMATICAL FORMULATION

Mathematical formulation of the problem has been considered for two cases, i.e., surface reaction inside a permeable tube and surface reaction without permeation.

Case-1: Surface Reaction inside a Permeable Tube

Based on the model proposed by Elliott *et al.* [9,10], Mansour [11] tried to solve a similar problem for absorption coupled with permeation through intestinal wall with circular cross-section. Considering very small permeation velocity compared to axial velocity, he neglected radial velocity term and took the equation for velocity profile the same as that for the laminar flow through pipes. Further, assuming very high absorption rate (sink condition), the surface concentration was taken to be zero all along the tube length. In the present paper, however, the reaction rate is assumed to be finite (i.e., the surface concentration is not zero) and a modified velocity profile is being used.

The velocity profile in a circular tube with constant wall permeability has been developed by several workers [12,13]. According to these approaches, the axial velocity (u) in case of low permeation rate can be given by

$$u = 2\langle u\rangle\left[1 - \frac{2v_{\mathrm{W}}x}{\langle u\rangle R}\right]\left[1 - \left(\frac{r}{R}\right)^2\right]. \tag{1}$$

Since the fluid velocity component in the radial direction (v) is several orders of magnitude smaller than that in the axial direction (u), therefore, the mathematical model for ATP transport inside a circular tube (equation of continuity for constant density and diffusivity) reduces to

$$2\langle u\rangle\left[1 - \frac{2v_{\mathrm{W}}x}{\langle u\rangle R}\right]\left[1 - \left(\frac{r}{R}\right)^2\right]\frac{\partial C}{\partial x} = D\left[\frac{\partial^2 C}{\partial r^2} + \frac{1}{r}\frac{\partial C}{\partial r}\right]. \tag{2}$$

The wall of the tube (at $r = R$), made of epithelial cell, provides a permeating as well as a reacting surface with first order chemical kinetics [7]. Hence, at the steady state, mass consumed at the surface in chemical reaction is equal to the sum of mass fluxes approaching the surface due to diffusion and convection. Thus we have

$$-D\left.\frac{\partial C}{\partial r}\right|_{r=R} + v_W C = kC. \tag{3}$$

This gives

$$\text{B.C. I:} \qquad \left.\frac{\partial C}{\partial r}\right|_{r=R} = -(k - v_W)C/D \quad \text{(for all } x\text{)}. \tag{4a}$$

The axisymmetric condition gives

$$\text{B.C. II:} \qquad \left.\frac{\partial C}{\partial r}\right|_{r=0} = 0 \quad \text{(for all } x\text{)} \tag{4b}$$

and for a uniform inlet concentration, we have

$$\text{B.C. III:} \qquad C = C_0 \text{ at } x = 0 \quad \text{(for all } r\text{)}. \tag{4c}$$

Using the dimensionless concentration c $(= C/C_0)$, radial distance γ $(= r/R)$ and by defining a dimensionless axial distance parameter $[\eta(x)]$ as

$$\eta = \ln\left[1 - \frac{2v_W x}{\langle u\rangle R}\right]^{-\alpha} \tag{5}$$

Eq. (2) reduces to

$$4(1-\gamma^2)\frac{\partial c}{\partial \eta} = \left[\frac{\partial^2 c}{\partial \gamma^2} + \frac{1}{r}\frac{\partial c}{\partial \gamma}\right]. \tag{6}$$

Here, it is noteworthy that η varies from 0 to ∞ as x varies from 0 to its upper limit (i.e., $\langle u\rangle R/2v_W$) where the total volume filtered becomes equal to the volumetric feed rate. The corresponding boundary

conditions (Eq. (4)) in dimensionless form become

$$\text{B.C. I:} \quad \left.\frac{\partial c}{\partial \gamma}\right|_{\gamma=1} = -(k - v_W)Rc/D = -\psi c \quad \text{(for all } \eta\text{)}, \tag{7a}$$

$$\text{B.C. II:} \quad \left.\frac{\partial c}{\partial \gamma}\right|_{\gamma=0} = 0 \quad \text{(for all } \eta\text{)} \tag{7b}$$

$$\text{B.C. III:} \quad c = 1 \text{ at } \eta = 0 \quad \text{(for all } \gamma\text{)}. \tag{7c}$$

The parameter ψ in Eq. (7a) is the modified Thiele modulus for coupled reaction–permeation problem.

The procedure for solving Eq. (6) along with boundary conditions (Eqs. (7)) are given in Appendix. As discussed in our earlier communication [4], the Thiele modulus (ϕ^2) is always positive whereas the modified Thiele modulus (ψ) in Eq. (7a) may be either positive or negative depending upon the value of k and v_W. The complete solution of Eq. (2) and associated boundary conditions becomes

$$\frac{C}{C_0} = \sum_{n=1}^{\infty} A_n \left[1 - \frac{2v_W x}{\langle u \rangle R}\right]^{\lambda_n^2 \alpha/4} \times \exp[-\lambda_n r^2/2R^2] M(1/2 - \lambda_n/4,\ 1,\ \lambda_n r^2/R^2), \tag{8}$$

where λ_n and A_n are nth eigenvalue and coefficient, respectively.

Case-2: Surface Reaction without Permeation

Equation (8) cannot be used for impermeable tubes since it becomes indeterminate when v_W is equated to zero. The velocity profile in case of impermeable tubes can be obtained by substituting $v_W = 0$ in Eq. (1). This gives the model equation for ATP transport as

$$2\langle u \rangle \left[1 - \left(\frac{r}{R}\right)^2\right] \frac{\partial C}{\partial x} = D\left[\frac{\partial^2 C}{\partial r^2} + \frac{1}{r}\frac{\partial C}{\partial r}\right]. \tag{9}$$

In the dimensionless form, Eq. (9) reduces to

$$4(1 - \gamma^2)\frac{\partial c}{\partial \xi} = \left[\frac{\partial^2 c}{\partial \gamma^2} + \frac{1}{r}\frac{\partial c}{\partial \gamma}\right] \tag{10}$$

where, ξ is the dimensionless axial distance $(2Dx/\langle u\rangle R^2)$ and the boundary conditions in dimensionless form become

$$\text{B.C. I:} \quad \left.\frac{\partial c}{\partial \gamma}\right|_{\gamma=1} = -\frac{kR}{D}c = -\phi^2 c \quad (\text{for all } \xi), \tag{11a}$$

$$\text{B.C. II:} \quad \left.\frac{\partial c}{\partial \gamma}\right|_{\gamma=0} = 0 \quad (\text{for all } \xi) \tag{11b}$$

and

$$\text{B.C. III:} \quad c = 1 \text{ at } \xi = 0 \quad (\text{for all } \gamma). \tag{11c}$$

The parameter ϕ^2 in Eq. (11a) is the well known Thiele modulus. Since the form of the differential equations (Eqs. (6) and (10)) and the boundary conditions (Eqs. (7) and (11)) are identical, hence the solution procedure for these equations are also identical to that explained in the Appendix. However, the concentration profile in case of impermeable tube is different from that expressed in Eq. (8) for permeable tubes. The concentration profile in this case becomes

$$\frac{C}{C_0} = \sum_{n=1}^{\infty} A_n \exp\left[-\frac{\lambda_n}{2R^2}\left(\frac{Dx}{\langle u\rangle} + r^2\right)\right] M(1/2 - \lambda_n/4,\ 1,\ \lambda_n r^2/R^2). \tag{12}$$

DISCUSSION

In the past, attempts have been made to obtain concentration profiles under similar conditions using different approaches. Mansour [11] solved similar problem for intestinal wall permeability (sink condition) by the method of Laplace transformation, Kumar *et al.* [4] obtained concentration profile in rectangular channel geometry using the present mass transfer model for ATP transport and Kumar [13] solved the present problem by using a computer simulator based on modified finite difference method [14].

Figure 1 shows the variation of dimensionless concentration in the bulk of liquid as a function of dimensionless radial distance (γ), by computer simulator [13,14], Laplace transformation [11] and the

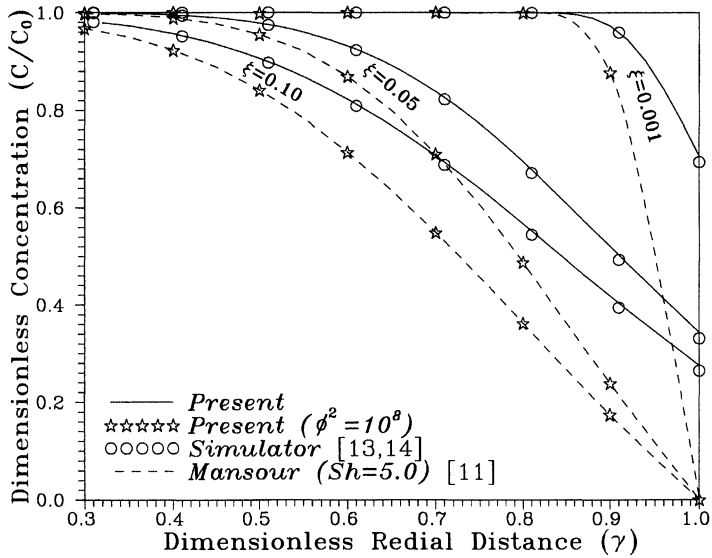

FIGURE 1 Comparison of ATP concentration in the bulk of liquid inside the tube calculated by three approaches at $\phi^2 = 5.0$.

present approach for $\phi^2 = 5$ and at various axial positions (ξ). Solid lines are obtained by the present solution given by Eq. (12) and the results obtained by a computer simulation [13,14] are shown as point values. Dotted lines are obtained by the solution proposed by Mansour [11] by substituting the value of dimensionless permeation ($v_W R/D$) equal to ϕ^2. This makes the B.C. I defined by Mansour [11] identical to Eq. (11a). It is observed that results of the present solution and the computer simulation are in excellent agreement whereas the concentration is always lower when diffusion controlled surface reaction (sink condition) is assumed. However, the concentration profile in the bulk of liquid obtained for the sink condition [11] is close to the values obtained by the present approach when the Thiele modulus is very large (i.e., $\phi^2 = 10^8$).

A comparison of the dimensionless wall concentration obtained by the computer simulator and analytical solution (using 50 eigenvalues) at $\phi^2 = 5$ and 20 is presented in Fig. 2 as a function of dimensionless axial position (ξ). Results obtained by two methods are in good agreement for larger values of ξ. For very small ξ ($< 3 \times 10^{-4}$), that comes to about 10–20 μm from the inlet end for practical situation,

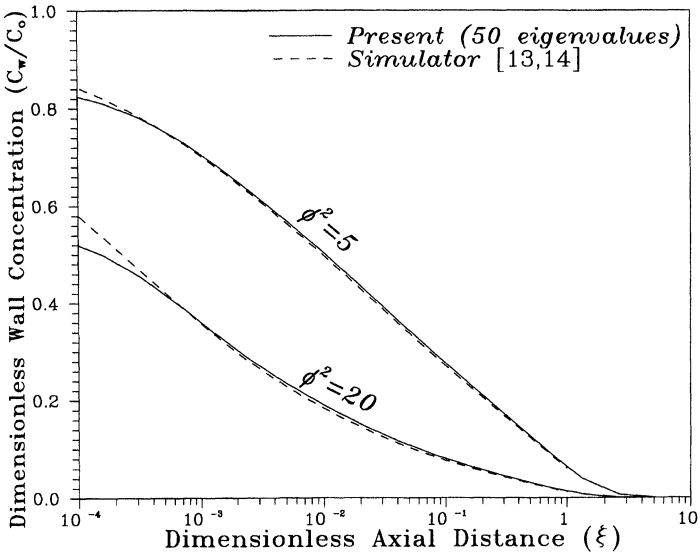

FIGURE 2 Dimensionless ATP concentration near the cell surface ($r = R$) in an impermeable tube as a function of axial distance ξ ($= 2Dx/\langle u \rangle R^2$).

analytical solution under predicts the wall concentration. This is due to the fact that analytical method requires even more eigenvalues in this region. Increase in the number of eigenvalues, however, does not lead to improvement in the results due to truncation and rounding off errors during computation.

The dimensionless wall concentration in case of surface reaction coupled with permeation and negative value of ψ ($= -0.1$), i.e., the case when rate of approach of ATP to the cell layer by convection is greater than the rate of consumption due to reaction, has been plotted in Figs. 3 and 4. These figures show that when the concentration is plotted against dimensionless distance ξ (Fig. 3), different lines for different values of α are obtained, whereas when the same concentration is plotted as a function of η (Fig. 4) we get only a single line from both analytical solution as well as the computer simulator (which is based on an entirely different approach). However, the computational time required for the computer simulator is about 50 times higher than that for analytical solution.

Figure 5 compares the dimensionless cytosolic Ca^{2+} concentration obtained by Dull and Davies [8] as a function of shear stress at

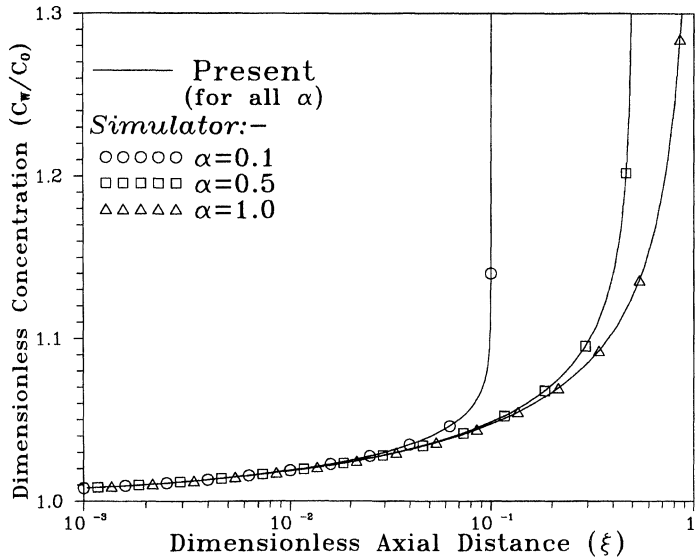

FIGURE 3 Dimensionless ATP concentration near the cell surface ($r = R$) in a permeable tube as a function of axial distance ξ ($= 2Dx/\langle u \rangle R^2$).

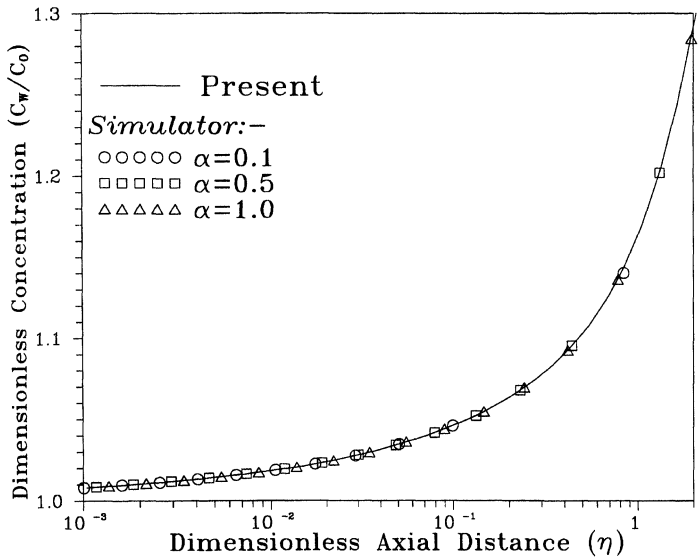

FIGURE 4 Dimensionless ATP concentration near the cell surface ($r = R$) in a permeable tube as a function of axial distance η.

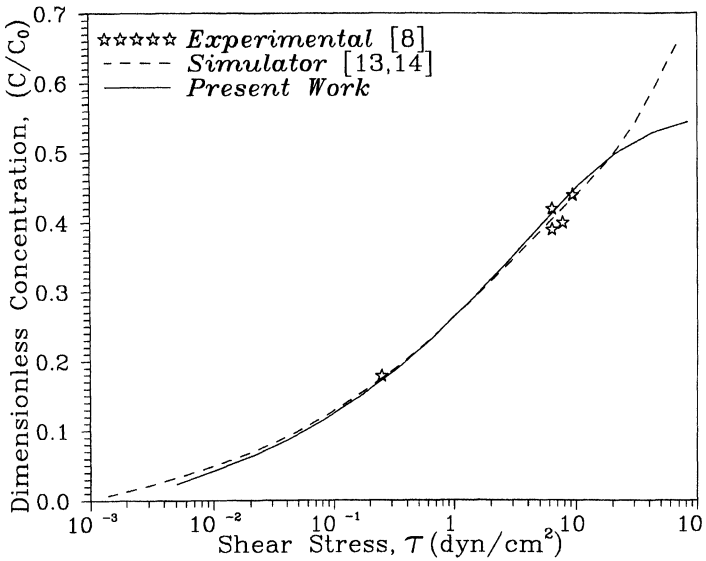

FIGURE 5 Comparison of experimental and predicted values of dimensionless ATP concentration near the cell surface ($r = R$) in an impermeable tube as a function of shear stress τ.

$\phi^2 = 20$. The details of obtaining dimensionless Ca^{2+} concentration are given in Kumar and Upadhyay [15] and the correlation for predicting shear stress in terms of ξ are given in Kumar *et al.* [4]. Within the range covered by the experiments, there is very good agreement between the experimental values of dimensionless cytosolic Ca^{2+} ion concentration and the extracellular ATP concentration predicted by using simulator and analytical methods.

CONCLUSIONS

In the present work solutions for the concentration profile in tubes with surface reaction coupled with permeation have been obtained in terms of confluent hypergeometric function. Due to the fast converging nature of this function, larger number of eigenvalues could be calculated compared to the other solution procedure such as power-series approach, leading to more accurate results.

A good comparison of the experimental and theoretical results of the intracellular Ca^{2+} concentration in the calf aorta endothelial cells

and the extracellular ATP concentration provides yet another example in support of the mass transfer model for intracellular calcium response of the endothelial cells.

NOMENCLATURE

A constant,
C concentration (g/ml),
C_0 feed concentration (g/ml),
c concentration $[C/C_0]$ (dimensionless),
D diffusivity of ATP in the solution (cm^2/s),
L axial distance ($2\ v_W x/\langle u\rangle R^2$) (dimensionless),
R radius of the tube (cm),
r radial distance measured from the axis of the tube (cm),
$\langle u\rangle$ volume average feed velocity (cm/s),
v_W permeation velocity (cm/s),
x axial distance measured from the tube inlet (cm).

Greek

α dimensionless parameter ($D/v_W R$),
γ dimensionless radial distance (r/R),
η axial distance, defined in Eq. (5) (dimensionless),
λ^2 eigenvalue,
ξ axial distance ($2\ Dx/\langle u\rangle R^2$) (dimensionless),
ϕ^2 Thiele modulus (kR/D) (dimensionless),
ψ modified Thiele modulus $[(k - v_W R/D]$ (dimensionless),

Subscript

n indicating parameter based on nth eigenvalue.

References

[1] A.J. Vander, J.H. Sherman and D.S. Luciano, *Human Physiology: The Mechanisms of Body Function*, Tata-McGraw-Hill, New Delhi (1981).
[2] D. Brown and J.L. Stow, "Protein trafficking and polarity in kidney epithelium: From cell biology to physiology", *Physiol. Rev.*, **76** (1996), 245–297.
[3] J.L. Sutko and J.A. Airey, "Ryanodine receptor Ca^{2+} release channels: Does diversity in form equal diversity in function", *Physiol. Rev.*, **76** (1996), 1027–1071.

[4] V. Kumar, R.N. Pandey and S.N. Upadhyay, "A closed form solution of convective mass transfer model for intracellular calcium response of endothelial cells", *Math. Probl. Eng.*, **4** (1998), 437–459.
[5] J.A. Frangos, S.G. Eskin, L.V. McIntire and C.L. Ives, "Flow effects on prostacyclin production by culture human endothelial cell", *Science*, **227** (1985), 1477–1479.
[6] M. Mo, S.G. Eskin and W.P. Schilling, "Flow induced changes in calcium signaling of vascular endothelial cells: Effect of shear stress and ATP", *Am. J. Physiol.*, **260** (Heart Circ. Physiol. 29) (1991) H1698–H1707.
[7] M.U. Nollert and L.V. McIntire, "Convective mass transfer effects on the intracellular calcium response of endothelial cells", *Trans. ASME (J. Biomech. Eng.)*, **114** (1992), 321–326.
[8] R.O. Dull and P.F. Davies, "Flow modulation of agonist (ATP) response (Ca^{++}) coupling in vascular endothelial cells", *Am. J. Physiol.*, **261**(1) Part 2 (1991), H149–H154.
[9] R.L. Elliot, "Intestinal absorption: Analysis of theoretical models", Ph.D. Thesis, University of Wisconsin (1979).
[10] R.L. Elliot, G.L. Amidon and E.N. Lightfoot, "A convective mass transfer model for determining intestinal wall permeabilities: Laminar flow in a circular tube", *J. Theor. Biol.*, **87** (1980), 757–771.
[11] A.R. Mansour, "An exact solution to a convective mass transfer laminar flow model for determination of intestinal wall permeabilities", *The Chem. Eng. J.*, **38** (1988), B29–B32.
[12] S.W. Yuan and A.B. Finkelstein, "Laminar pipe flow with injection and suction through a porous wall", *Trans. ASME*, **78** (1956), 719–724.
[13] V. Kumar, "Mathematical modelling and computer simulation of membrane processes involving synthetic and natural membranes", Ph.D. Thesis, Department of Chemical Engineering, Banaras Hindu University, Varanasi (1995).
[14] V. Kumar and S.N. Upadhyay, "Computer simulation of membrane processes: Ultrafiltration and dialysis units" (unpublished results).
[15] V. Kumar and S.N. Upadhyay, "Mass transfer based model predicts endothelial cell response" (unpublished results).
[16] L.J. Slater, *Confluent Hypergeometric Functions*, The Synodics of the Cambridge University Press (1960).

APPENDIX

Equations (6) and (10) are of the form:

$$4(1-\gamma^2)\frac{\partial c}{\partial \chi} = \frac{\partial^2 c}{\partial \gamma^2} + \frac{1}{\gamma}\frac{\partial c}{\partial \gamma}, \tag{A.1}$$

where χ may be either η (Eq. (6)) or ξ (Eq. (10)) and boundary condition in dimensionless form are:

$$\text{B.C. I}: \quad \left.\frac{\partial c}{\partial \gamma}\right|_{\gamma=1} = -\theta c \quad (\text{for all } \chi), \tag{A.2}$$

$$\text{B.C. II:} \quad \left.\frac{\partial c}{\partial \gamma}\right|_{\gamma=0} = 0 \quad \text{(for all } \chi\text{)} \tag{A.3}$$

and

$$\text{B.C. III:} \quad c = 1 \text{ at } \chi = 0 \quad \text{(for all } \gamma\text{)}. \tag{A.4}$$

where θ may be either the Thiele modulus (ϕ^2) or the modified Thiele modulus (ψ).

To solve Eq. (A.1) along with boundary conditions (A.2)–(A.4) by the method of separation of variables it is assumed that

$$c = X(\chi) \cdot Y(\gamma). \tag{A.5}$$

Substituting in Eq. (A.1) we get two simultaneous differential equations:

$$\frac{d^2Y}{d\gamma^2} + \frac{1}{\gamma}\frac{dY}{d\gamma} + \lambda^2(1-\gamma^2)Y = 0 \tag{A.6}$$

and

$$\frac{dX}{d\chi} = -\frac{\lambda^2 X}{4}. \tag{A.7}$$

The solution of Eq. (A.7) is

$$X = B \exp(-\lambda^2\chi/4), \tag{A.8}$$

whereas Eq. (A.2) can be transformed to the confluent hypergeometric equation:

$$z\frac{d^2\omega}{dz^2} + (b-z)\frac{d\omega}{dz} - a\omega = 0 \tag{A.9}$$

by two transformations

$$z = \lambda\gamma^2 \tag{A.10}$$

and

$$\omega = Ye^{z/2}, \tag{A.11}$$

where $a = (1/2 - \lambda/4)$ and $b = 1$.

Equation (A.9) is the well known confluent hypergeometric equation (Kummer's equation) and its solution is

$$\omega = A_1 M(a, b, z) + A_2 U(a, b, z). \tag{A.12}$$

The first confluent hypergeometric function is

$$M(a, b, x) = \sum_{n=0}^{\infty} \frac{(a)_n}{(b)_n n!} x^n, \tag{A.13}$$

where $(a)_n = a(a+1)(a+2)\cdots(a+n-1)$ and $(a)_0 = 1$.

When b is equal to unity, the second hypergeometric function, which is a multi-valued function [16], can be given by

$$U(a, 1, z) = M(a, 1, z)\ \ln(z) + \sum_{m=1}^{\infty} \frac{(a)_m z^m}{(m!)^2}$$
$$\left[\frac{1}{a} + \cdots + \frac{1}{a+m-1} - \left(\frac{2}{1} + \cdots + \frac{2}{m}\right)\right]. \tag{A.14}$$

Thus the complete solution of Eq. (A.9) becomes

$$\omega = A_1 M(a, 1, z) + A_2 \Bigg[M(a, 1, z)\ \ln(z)$$
$$+ \sum_{m=1}^{\infty} \frac{(a)_m z^m}{(m!)^2} \left\{\frac{1}{a} + \cdots + \frac{1}{a+m-1} - \left(\frac{2}{1} + \cdots + \frac{2}{m}\right)\right\}\Bigg]. \tag{A.15}$$

Now, B.C. II in terms of ω and z becomes

$$\left[\sqrt{z}\left\{\frac{\mathrm{d}\omega}{\mathrm{d}z} - \frac{\omega}{2}\right\}\right]_{z=0} = 0. \tag{A.16}$$

Substituting the value of ω from Eq. (A.15) and taking the limiting case when z is tending to zero, we get

$$A_1 0 + A_2 \lim_{z \to 0} \left[\left(a - \frac{1}{2}\right)\sqrt{z}\ \ln(z) + \frac{1}{\sqrt{z}}\right] = 0. \tag{A.17}$$

The limiting value of the term inside the parenthesis at the left hand side of Eq. (A.17) becomes infinity as z tends to zero. Therefore, to satisfy Eq. (A.17), and hence the B.C. II, A_2 should be zero.

Thus the complete solution of Eq. (A.9) reduces to

$$\omega = A_1 M(a, 1, z). \tag{A.18}$$

Again, from B.C. I (Eq. (A.2)) in terms of ω and z we have

$$2\lambda \left.\frac{d\omega}{dz}\right|_{z=\lambda} + (\theta - \lambda)\omega(\lambda) = 0. \tag{A.19}$$

Substituting the value of ω from Eq. (A.18) we get

$$A_1[2a\lambda M(a+1, 2, \lambda) + (\theta - \lambda)M(a, 1, \lambda)] = 0. \tag{A.20}$$

Since $A_1 \neq 0$, therefore we get the characteristic equation as

$$2a\lambda M(a+1, 2, \lambda) + (\theta - \lambda)M(a, 1, \lambda) = 0. \tag{A.21}$$

Roots of the characteristic equation give eigenvalues (λ_n). About 50 eigenvalues for different values of ψ were calculated. A few of them at each ψ are given in Table AI.

Now, from Eqs. (A.11) and (A.18) we get the eigenfunction as

$$Y_n = M(a_n, 1, z_n)e^{-z_n/2}. \tag{A.22}$$

Since Eq. (A.6) along with B.C. I and B.C. II constitutes a Sturm–Liouville problem, eigenvalues λ_n and eigenfunction Y_n form an orthogonal set with respect to the weight function $\gamma(1-\gamma^2)$ over the interval [0, 1], i.e.,

$$\begin{aligned} \int_0^1 \gamma(1-\gamma^2) Y_m Y_n \, d\gamma = 0 \quad &\text{when } m \neq n \text{ and} \\ \neq 0 \quad &\text{when } m = n. \end{aligned} \tag{A.23}$$

Therefore by using B.C. III and Eq. (A.23) we get

$$A_n = \frac{\int_0^1 \gamma(1-\gamma^2) Y_n \, d\gamma}{\int_0^1 \gamma(1-\gamma^2) Y_n^2 \, d\gamma}. \tag{A.24}$$

TABLE AI Eigenvalues (λ_n^2) of the characteristic Eq. (A.21)

n	$\psi=-1.0$	$\psi=-0.5$	$\psi=-0.1$	$\psi=0.0$	$\psi=1.0$	$\psi=5.0$
1	−6.7706828986	−2.5596979050	−0.4190518057	0.0000000000	2.6937005129	5.5538125137
2	20.0695276514	22.9635444484	25.1620046365	25.6796120019	30.0118690516	37.6387130070
3	77.5100738805	80.8100629244	83.2748042755	83.8617554592	89.0374059300	100.2697156971
4	167.2938392397	170.8523569574	173.5251752891	174.1667407073	179.9687419417	194.0939317643
5	289.2306883771	293.0000955772	295.8488116905	296.5362993478	302.8501813956	319.4010594266
6	443.2637564637	447.2166997813	450.2196443254	450.9471942141	457.6999926721	476.3477172332
7	629.3651878452	633.4827057986	636.6239954172	637.3873367699	644.5276755063	665.0283023531
8	847.5185161835	851.7862746234	855.0536439237	855.8494988340	863.3388663011	885.5041254131
9	1097.7129662899	1102.1195766344	1105.5032034351	1106.3289611109	1114.1372118353	1137.8172705051
10	1379.9410105118	1384.4771226121	1387.9689253557	1388.8224476066	1396.9252215275	1421.9978857883
⋮	⋮	⋮	⋮	⋮	⋮	⋮
50	38917.5167467823	38924.8253661392	38930.5596631684	38931.9796897651	38946.0064610398	38997.6257696089
n	$\psi=10.0$	$\psi=20.0$	$\psi=50.0$	$\psi=75.0$	$\psi=100.0$	$\psi=1.0\text{E}+08$
1	6.3340430079	6.7958725173	7.0994133488	7.1697297104	7.2052884996	7.3135868061
2	40.5080609495	42.3781562564	43.6707190128	43.9766378370	44.1322085790	44.6094606162
3	105.4869575671	109.2022330429	111.9021403290	112.5551375716	112.8890900254	113.9210297087
4	201.6457879700	207.4408787442	211.8508486723	212.9394378166	213.4991420139	215.2405414715
5	329.1924485146	337.1971034313	343.5512670959	345.1502343742	345.9765363034	348.5641127655
6	488.2607377307	498.5430232796	507.0284022229	509.2028877539	510.3320668280	513.8900569370
7	678.9433783280	691.5328019898	702.3016381297	705.1094320275	706.5742927123	711.2175278265
8	901.3078073469	916.2089255223	929.3866406795	932.8796500142	934.7102138249	940.5460504472
9	1155.4048240212	1172.6057352367	1188.2964545708	1192.5217189743	1194.7457002247	1201.8753350817
10	1441.2737471401	1460.7516106697	1479.0421881980	1484.0426232451	1486.6857751192	1495.2051935598
⋮	⋮	⋮	⋮	⋮	⋮	⋮
50	39052.6688788417	39136.6415353231	39269.3523439014	39320.9474831090	39351.6925513494	39468.4996137535

Details for finding the values of integrals in Eq. (A.24) are given elsewhere [4], which gives

$$A_n = \frac{\theta Y_n(1)}{\theta Y_n^2(1) + \int_0^1 \gamma(\mathrm{d}Y_n/\mathrm{d}\gamma)^2 \mathrm{d}\gamma}, \tag{A.25}$$

where

$$Y_n(1) = M(a_n, 1, \lambda_n)\mathrm{e}^{-\lambda_n/2} \tag{A.26}$$

and

$$\frac{\mathrm{d}Y_n}{\mathrm{d}\gamma} = 2\lambda_n\gamma\mathrm{e}^{-\lambda_n/2}\left[M(a_n + 1, 2, \lambda_n\gamma^2)a_n - \frac{M(a_n, 1, \lambda_n\gamma^2)}{2}\right]. \tag{A.27}$$

To evaluate A_n using Eq. (A.25), Eq. (A.27) was integrated numerically by Simpson's 1/3 rule.